DOI: 10.31577/ahs-2025-0026.02.0032

ACTA HYDROLOGICA SLOVACA

Volume 26, No. 2, 2025, 318 – 326

Estimation of actual evapotranspiration in a mountain catchment using distributed hydrological models and satellite data

Patrik SLEZIAK*, Michal DANKO, Martin JANČO, Ladislav HOLKO, Viera RATTAYOVÁ

Actual evapotranspiration (AET) is one of the fundamental components of the water balance. At the catchment scale, it is typically determined from the hydrological balance or by modelling. Vegetation changes, such as forest dieback or forest harvesting, can significantly affect the AET, but the extent of these changes is not well known. This work aims to (a) compare the AET calculated using two different modelling approaches and satellite data in a mountain catchment (the Jalovecký Creek catchment in the West Tatras) that is undergoing natural dieback and forest regeneration, and (b) evaluate changes in the water balance of the catchment. Satellite evapotranspiration datasets (GLEAM versions 3.5b and 4.2a, GLDAS) and reanalysis-based products (ERA5 and MERRA-2) were utilized. Two distributed hydrological models, WaSiM and MIKE SHE, were used to model the AET. Daily data (precipitation, air temperature, air humidity, wind speed, solar radiation) from hydrological years 2013 (original forest state) to 2022 (altered forest) were used as input data for the models. The calculation of potential evapotranspiration (PET) in the WaSiM model is based on the Penman-Monteith method, while the MIKE SHE model uses the Blaney-Criddle method. Each model has a parameterization allowing the calculation of AET for the vegetation classes present in the study catchment (spruce forest, dwarf pine, alpine meadows). Due to the ongoing forest dieback and regeneration, the models were deliberately calibrated for each year of the study period. The results showed that both models overestimated the average annual AET calculated from measured precipitation and runoff. The highest AET values were simulated for the spruce forest, the lowest for the alpine meadows. AET estimates derived from the reanalyses and satellite products exhibited reduced interannual variability compared to that based on the hydrological balance. ERA5 systematically underestimated monthly AET by up to 40% in comparison with other datasets, whereas MERRA2 consistently yielded values at the upper range, exceeding ERA5 by approximately 30–40% during summer.

KEY WORDS: water balance, vegetation zones, hydrological modelling, remote sensing datasets, mountain environment

Introduction

It is well known that human activities impact the hydrological cycle. Monitoring of the long-term regime of hydrological balance at the basin level can help identify such changes. Evapotranspiration is a major component of the hydrological balance, and also a significant element of the energy balance. Actual evapotranspiration (AET) characterizes the amount of water evaporated at a given location under local meteorological conditions and is tied to the current water availability. Its reliable estimation is important for the assessment and use of water resources, management of the water needs of crops, predicting and monitoring drought, climatological studies, etc. While the point measurement of the AET is possible, its estimation at the catchment scale has to rely on calculations. A standard method for AET calculation is the hydrological balance (precipitation-runoff) which is suitable especially for the obtaining of the long-term averages (Duethmann and Blöschl, 2018; Pekárová et al., 2023). Indirect methods of AET calculation are mainly related to the use of remote sensing (Zhang et al., 2010; Gao et al., 2010; Reichle et al., 2011; Somorowska, 2022) and hydrological models (Parajka et al., 2004; Huang et al., 2020). Hydrological models utilize different approaches to the AET calculation, and their results are not often compared. The number of publicly available remote sensing datasets of evapotranspiration and its components has been increasing in the last decades (e.g. Reichle et al., 2011; Somorowska, 2022; Miralles et al., 2011; Talsma et al., 2018; Yan et al., 2020). It enabled the expansion of evapotranspiration research to areas where no measured data are available (Zhang et al., 2016). The primary advantage of the evapotranspiration estimates based on satellite data is their inherent spatial nature. Studies comparing various remote sensing-based datasets across different altitudes, climatic zones, and

land cover types highlight varying performance of the evapotranspiration estimates (e.g., Talsma et al., 2018; Salazar-Martínez et al., 2022).
This study compares the AET obtained from two distributed hydrological models: WaSiM (Schulla, 1997; 2019) and MIKE SHE (MIKE by DHI, 2011) with data obtained from the remote sensing and reanalysis in a small mountain catchment undergoing forest changes.

Study area and data

The Jalovecký Creek catchment is a small mountain catchment located in the Western Tatra Mountains (Fig. 1). Its area is 22.2 km², with a length of approximately 7 km in the north-south direction. The catchment is characterised by significant elevation differences (816–2178 m above sea level) with an average elevation of 1500 m above sea level. The average slope of the catchment is 30°, and most of the slopes have a southeast orientation. Almost half of the catchment (44%) is covered by spruce forest, where dieback began in 2012. Since then, about 25% of the original spruce cover has changed, creating an opportunity to compare various characteristics (e.g., rainfall interception, surface runoff, leaf area index, etc.) between dead spruce stands (where regeneration has already begun) and living ones (Jančo et al., 2024). The remaining 31% and 25% of the catchment are covered by the dwarf pine, and alpine meadows/bare rocks. The bedrock is composed of gneiss and crystalline schists (approximately 48% of the basin area), granite (21%), covered at some places by Quaternary sediments (24%). The remaining 7% of the basin is formed by Mesozoic rocks (limestone and dolomite). Cambisols, podzols, and lithosols represent the maim soil types.

Methods

For this study, two hydrological models were used: WaSiM (Schulla, 1997; 2019) and MIKE SHE (MIKE by DHI; 2011). The results of AET modelling were compared with five evapotranspiration datasets, including observation-driven products based on remote sensing data and land surface modelling (GLEAM versions 3.5b and 4.2a, and GLDAS) as well as reanalysis-based products (ERA5 and MERRA-2).

Distributed hydrological models

The **WaSiM model** ("Water flow and balance SIMulation model", Schulla, 1997, 2019) is a distributed hydrological model developed for small mountain basins. The minimum requirement for meteorological input data is a time series of precipitation and air temperatures in a daily or shorter time step from at least one meteorological station. In our case, we used daily time series of precipitation (8 stations), air temperature (3 stations), wind speed (2 stations), air humidity (2 stations) and global radiation (2 stations) from hydrological years 2013 (representing the original forest state) to 2022 (altered forest). Spatial maps were created from the daily time series on each day. The spatial distribution of precipitation was calculated using a combination of the inverse distance and the altitude gradient interpolation methods. The spatial distribution of air temperature was calculated using the altitude gradient. We used the inverse distance method to calculate the spatial distribution of wind speed, air humidity and global radiation. Additional model inputs were represented by raster maps of (resolution of 50 m) of elevation and relief characteristics derived from it, vegetation cover and soil types.

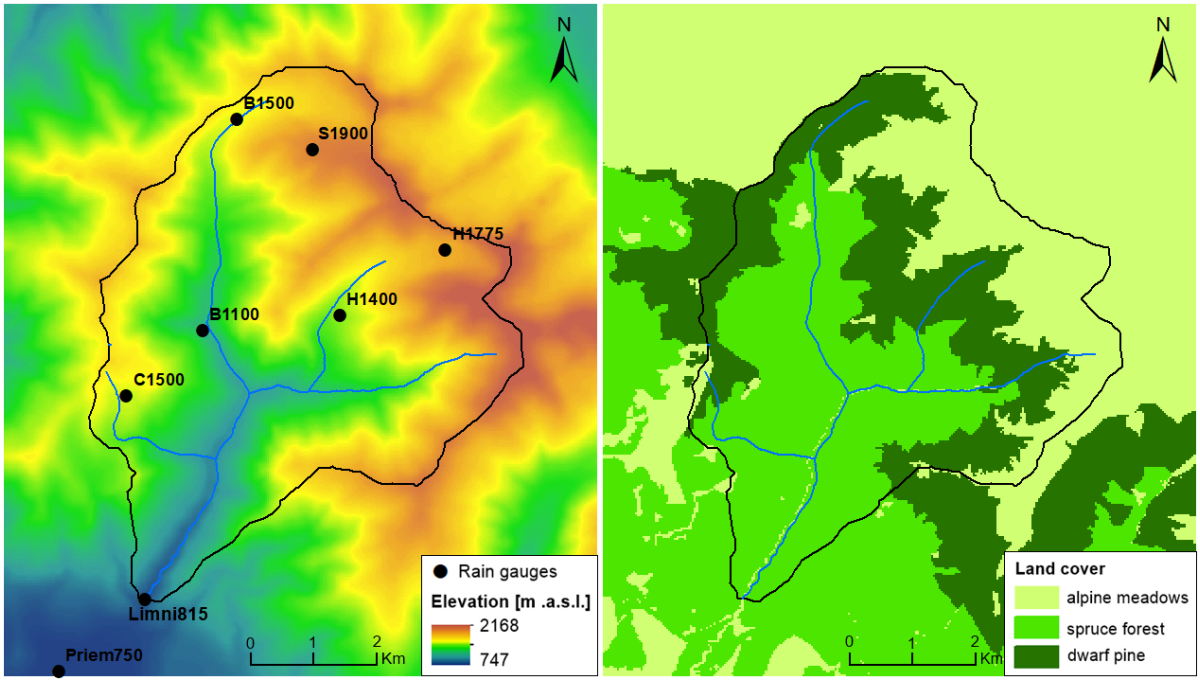


Fig. 1. Topography (left) and land cover (right) of the studied Jalovecký Creek catchment. The black points are locations with precipitation measurements.

The Penman-Monteith method (Monteith, 1975) was used to calculate the potential evapotranspiration. The following parameters are used to parameterize the potential evapotranspiration: surface resistivity, leaf area index, and root zone depth. The actual evapotranspiration is calculated by reducing potential evapotranspiration according to soil moisture. In this study, we did not change the vegetation parameters because we first wanted to determine how does the simulated actual evapotranspiration (AET) compare to the AET obtained from the hydrological balance, what is the interannual variability of the simulated AET, and whether poorer simulation results (evapotranspiration, runoff) in specific periods might indicate the influence of forest changes. The model was calibrated for each hydrological year separately against the measured snow water value from site C1500 (Fig. 1) representing the average elevation of the catchment and the discharge measured at catchment outlet (Limni815 in Fig. 1). We have first calibrated the snow parameters of the model, and then the parameters affecting soil moisture and runoff. Automatic parameter optimization using the PEST method (Doherty, 2016) was used. The correlation coefficient and sum of squares of deviations between the measured and simulated values were used as the optimization functions during calibration.

The **MIKE SHE** model is a spatially distributed hydrological model (MIKE by DHI, 2011) that can operate at daily or shorter time steps. The maps of daily precipitation and air temperature, prepared by the WaSiM model were used as input meteorological data. The geospatial data consisted of the digital terrain model, land use and soil characteristics (Hlaváčiková et al., 2014) maps. Potential evapotranspiration was calculated using the Blaney-Cridle method (Schrödter, 1985). Parameterization of the actual evapotranspiration was used the crop-specific coefficients for spruce forest, dwarf pine, and alpine meadows. The model parameters were obtained by automatic optimization using the SCE method (Shuffled Complex Evolution, Duan et al., 1993). We used the root mean square error (RMSE) as the optimization function. As with the WaSiM model, measurements of the snow water equivalent and discharge were used for calibration.

Remote sensing datasets

ERA5 is the fifth-generation gridded dataset of global climate and meteorological reanalysis data produced by the European Centre for Medium-Range Weather Forecasts (ECMWF). The dataset is available at an hourly temporal resolution and a spatial resolution of 0.25° (about 25 km in the study area), with evapotranspiration provided in meters of water equivalent. The algorithm is based on the ERA-Interim version, whose updates ceased in August 2019. ERA-Interim was routinely used as input for the WMO's annual climate state reports (Dee et al., 2011), incorporating numerous improvements. The most significant enhancement in the atmospheric modelling scheme, particularly regarding radiation, was the adoption of a more advanced Morcrette radiation model, replacing the older method based on neural networks (Dee et al., 2011).

MERRA-2 (Modern-Era Retrospective Analysis for Research and Applications) is a reanalysis of atmospheric data from the ERA satellite system, operated by NASA. It uses an updated version of the Goddard Earth Observing System (GEOS), which includes data from new microwave sensors and hyperspectral infrared radiometric instruments. Compared to the original MERRA, MERRA-2 incorporates the assimilation of satellite observations, enhanced representation of the cryosphere and ozone, and reduced false trends in precipitation resulting from changes in observation systems (Gelaro et al., 2017). Further changes in MERRA-2 involved new approaches to atmospheric water balance (Takacs et al., 2016), which led to a reduction in deviations and imbalances in components of the hydrological cycle. The MERRA-2 dataset used in this study is an hourly time-averaged reanalysis of land evapotranspiration [kg m^{-2} s^{-1}], comprising of land surface diagnostics at a spatial resolution of 0.625°×0.5° (Global Modeling and Assimilation Office, 2015).

The **GLEAM** model (Global Land Evaporation Amsterdam Model) is based on the Priestley–Taylor algorithm for calculating evapotranspiration and designed to use the satellite-derived observations to produce a spatially coherent estimate of evapotranspiration (Miralles et al., 2011). The main inputs to the model include satellite-derived data on the net radiation, precipitation, soil moisture, land surface and air temperatures, vegetation optical depth, and snow water equivalent. These data are sourced from various satellite platforms and complemented by a statistical information about the land surface and vegetation characteristics. GLEAM v3.5b is an older version that is primarily based on satellite data; the newer GLEAM v4.1a, available since July 2024, integrates both satellite and reanalysis data. Modelled results are available at a 0.25° (about 25 km) spatial resolution and daily time step, with data expressed in millimetres per day. Overall, the GLEAM 4.2a is considered more accurate for regional analyses, while the GLEAM 3.5b is preferred for its long-term consistency (Miralles et al., 2011).

GLDAS Noah (NASA Global Land Data Assimilation System, Version 2) is a model that provides gridded datasets with a spatial resolution of 0.25°×0.25°, available at various temporal resolutions. It contains the estimates of numerous variables characterizing the land surface and energy fluxes. It is based on the satellite observations, as well as direct measurements, utilizing advanced modelling and assimilation techniques (Rodell et al., 2004). The monthly GLDAS Noah dataset used in this study is generated by averaging the product available at a 3-hour time step and the evapotranspiration is provided in kg m^{-2} s^{-1} (Rui and Beaudoing, 2020).

Results and discussion

Hydrological modelling – comparison of the water balance components

A comparison of measured and simulated runoff obtained by simulations of the two models in the period of hydrological years 2013–2022 is presented in Table 1 and Fig. 2. Measured (interpolated) mean annual precipitation and runoff over the study period were 1626 mm and 1061 mm, respectively (=> AET = 565 mm). Both models only slightly underestimated measured mean annual runoff (WaSiM by 4%, MIKE SHE by 1%), but the differences in individual years were much larger (from -20% to +8% for WaSiM and from -13% to +17% for MIKE SHE). The largest differences between measured and simulated runoff were obtained for the hydrological years 2015–2017 (2018), that coincide with large changes in the forest although it is uncertain whether this was the reason of the differences.
The obtained NSE coefficients (Nash and Sutcliffe, 1970) do not differ much (NSE for WaSiM: 0.53–0.88; NSE for MIKE SHE: 0.55–0.91), which indicates a similar behavior of the models (Fig. 3).

Simulated actual evapotranspiration

Fig. 4 shows simulated annual actual evapotranspiration (AET) in the three vegetation zones present in the catchment (spruce forest, dwarf pine, alpine meadows). The two models simulated quite a different average annual AET for the zone of alpine meadows (61 mm from WaSiM, 136 mm from MIKE SHE). The differences for other two zones were smaller (184mm/206mm for the dwarf pine zone and 350 mm /335 mm for the spruce forest (WaSiM/MIKE SHE)).
Average annual simulated AET was greater than the AET calculated from measured precipitation and runoff (by 10% and 30% for WaSiM and MIKE SHE, respectively. The interannual variability of the simulated AET was small for both models. This does not correspond to the variability obtained from the water balance equation. The results obtained by the MIKE SHE model indicate a larger variability in the annual AET from the three vegetation zones (spruce forest, dwarf pine, alpine meadows), which is, however, relatively small. The simulated long-term average annual spatial distribution of AET obtained by the WaSiM and MIKE SHE models (Fig. 5) reflects the distribution

Table 1. **Measured (interpolated) annual precipitation and runoff (*Qobs*) in the Jalovecký Creek catchment. *Qsim* WaSiM and *Qsim* MIKE SHE are simulated runoff values obtained by two hydrological models**

Hydrological year	*P* [mm]	*Qobs* [mm]	*Qsim* WaSiM [mm]	*Qsim* MIKE SHE [mm]
2013	1439	703	759	678
2014	1851	1261	1241	1286
2015	1272	904	722	784
2016	1504	1079	965	934
2017	2103	1495	1325	1381
2018	1559	1109	1186	1103
2019	1465	979	873	1080
2020	2098	1155	1220	1349
2021	1458	987	980	1011
2022	1514	934	902	937

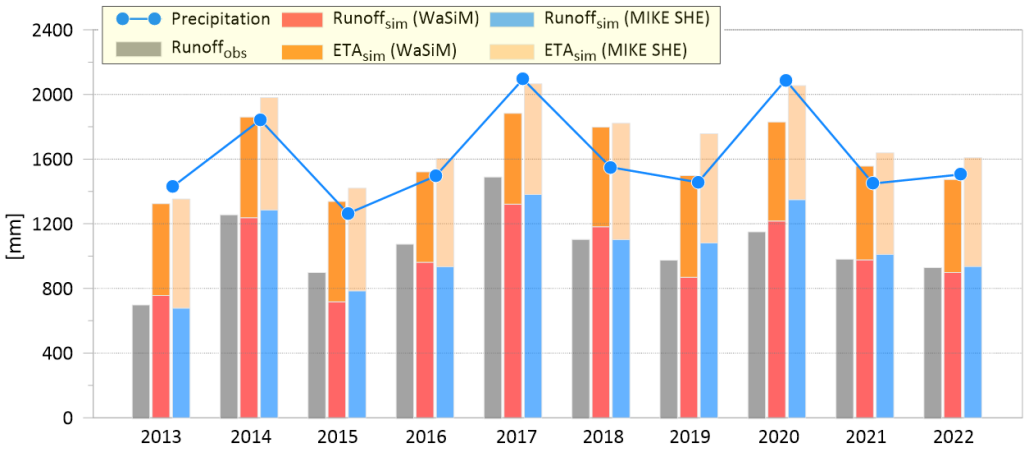


Fig. 2. Precipitation, runoff and actual evapotranspiration in hydrological years 2013–2022.

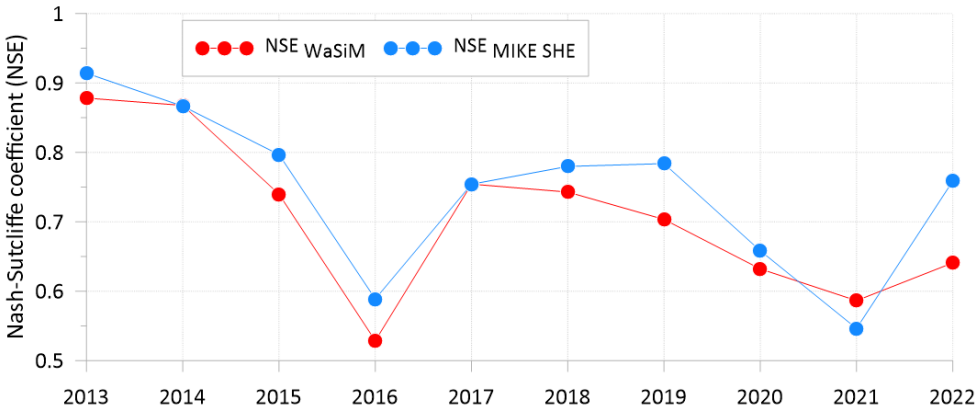


Fig. 3. Nash-Sutcliffe coefficient (NSE) expressing the relationship between measured and simulated runoff using two hydrological models (WaSiM vs. MIKE SHE).

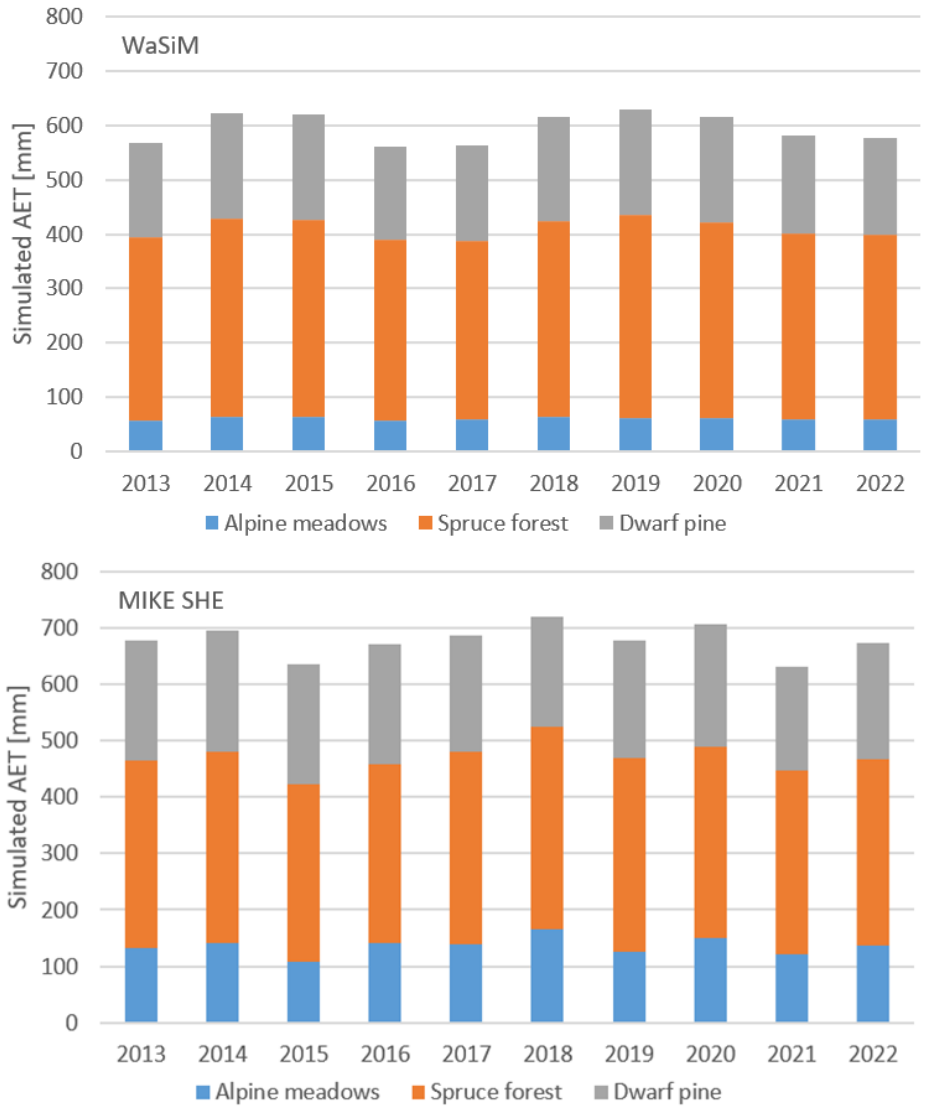


Fig. 4. Comparison of simulated annual actual evapotranspiration (AET) for three vegetation classes (spruce forest, dwarf pine, alpine meadows). The simulations were obtained using the WaSiM (top panel) and MIKE SHE (bottom panel) models.

of topography and vegetation cover. The highest AET values were simulated for the spruce forest, the lowest for the alpine meadows. Table 2 shows that WaSiM simulated very low AET for pixels in the alpine meadows

zone and moderate values for pixels in the dwarf pine and forest zones, whereas MIKE SHE provided higher AET that mostly varied between 100 and 150 mm for the alpine meadows zone, 150–250 mm for the dwarf pine zone and 300–350 mm for the forest zone. Annual evapotranspiration in the spruce forest measured in the Czech Republic by Kantor (1984) was 487 mm. Hu et al. (2024) concluded that mean annual evapotranspiration of alpine meadows in the Qinghai-Tibet Plateau was 347 mm. Annual evapotranspiration and sublimation of the sub-alpine Qinghai spruce forest in the same region was 417 mm (Zhu et al., 2014) while Nakai et al. (2013) reported 207 mm for the black spruce boreal forest in Alaska. Those values are closed to the values obtained from the MIKE SHE although the values simulated by the WaSiM model for the dwarf pine and forest zones may be reasonable as well. On the other hand, Fig. 5 suggests that the highest mean annual AET in the forest zone provided by the MIKE SHE occurred on the slopes with northern slopes that does not look reasonable. WaSiM simulated the highest mean annual AET in the forest on the slopes with south-eastern orientation that is more realistic.

Comparison of simulated actual evapotranspiration with satellite data

The course of annual values of actual evapotranspiration (AET) obtained from the simulations and various satellite datasets is shown in Fig. 6. Over the period 2013–2022, AET values from the hydrological models and reanalysis/satellite datasets exhibit smaller interannual variability compared to the AET obtained from the hydrological balance. The lowest AET values in every year were obtained from the ERA5 dataset. Conversely, the highest values were obtained from the MERRA-2 dataset. Differences from the values obtained from the hydrological balance ranged from -45.7% (ERA5 in 2020) to +89.3% (MERRA2 in 2015). In most years, the MIKE-SHE model produced higher AET values, while WASIM showed slightly lower but still overestimated results compared to the hydrological balance.

A comparison of the seasonal course of average monthly AET shows small differences in November to February and large differences in May to August. (Fig. 7). The highest differences were obtained for June and July.

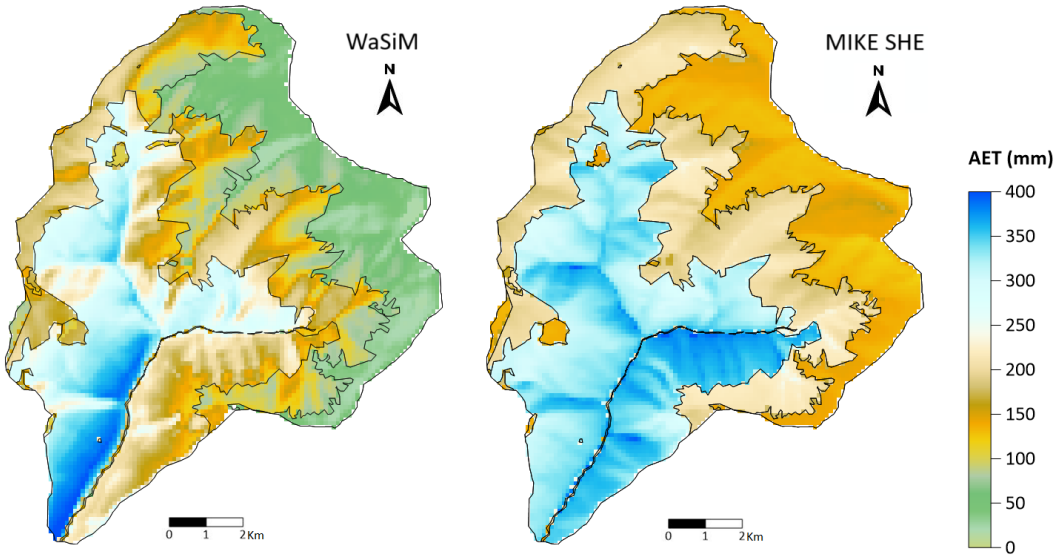


Fig. 5. Spatial distribution of the simulated average annual actual evapotranspiration (AET).

Table 2. Percentage of pixels in each vegetation zone with simulated mean annual AET between less than 50 mm and more than 400 mm

AET [mm]	WaSiM meadows [%]	WaSiM dwarf pine [%]	WaSiM forest [%]	MIKE SHE meadows [%]	MIKE SHE dwarf pine [%]	MIKE SHE forest [%]
below 50	52	1	0	0	0	0
50–100	42	25	0	0	0	0
100–150	3	32	7	92	0	0
150–200	3	37	19	7	41	0
200–250	0	5	22	1	59	0
250–300	0	0	20	0	0	5
300–350	0	0	22	0	0	68
350–400	0	0	11	0	0	26
above 400	0	0	0	0	0	0

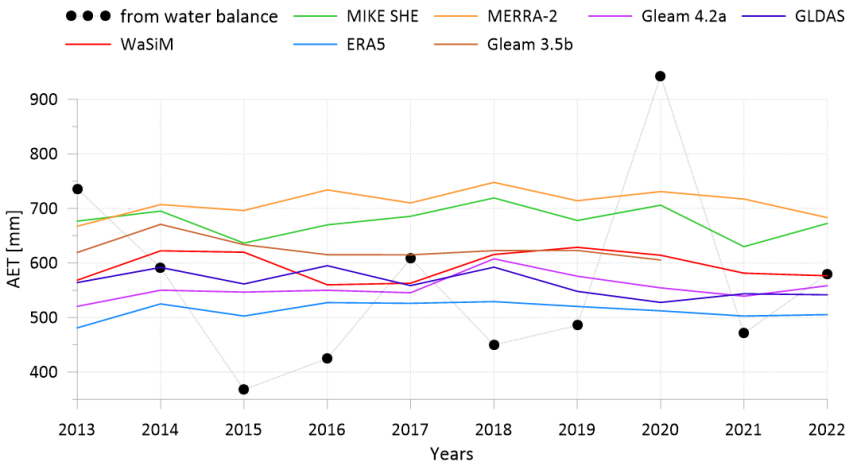


Fig. 6. The course of average annual values of AET simulated by the hydrological models and given by the reanalyses and satellite datasets.

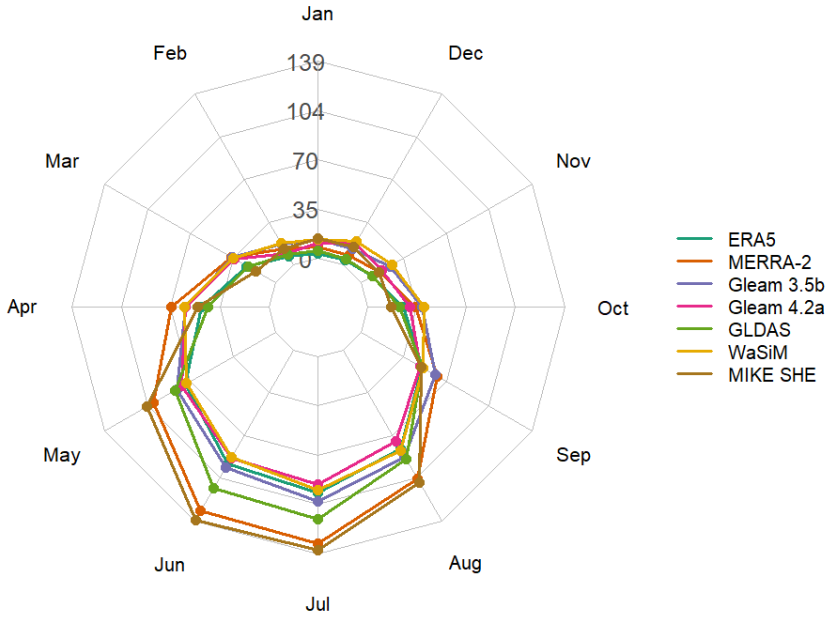


Fig. 7. The course of average annual values of actual evapotranspiration calculated using two models and from different satellite datasets.

The general monthly pattern indicates that in winter (December–February), ERA5 and GLDAS estimate about 40–70% lower AET than hydrological models, while MERRA2 and GLEAM products are closer but still 20–40% lower. In spring (March–May), ERA5 remains the lowest, with values about 20–30% below those of GLEAM and the models. MERRA2 and MIKE are the highest, exceeding ERA5 by up to 40% in May. In the summer months (June–August), evapotranspiration peaks, with MIKE and MERRA2 producing the largest values, approximately 30–40% higher than those of ERA5 and 10–20% higher than those of GLEAM. In autumn (September–November), the differences narrow, with ERA5 and GLDAS still 10–25% lower than GLEAM and models.

GLEAM is widely used in scientific and engineering applications. It often provided inputs for hydrological modelling (Jin and Jin, 2020) and drought assessment (Ma et al., 2023). Somorowska (2022) applied GLEAM to assess evapotranspiration in Poland, though no validation with observational data was conducted. Knist et al. (2017) compared GLEAM and ERA-Interim against RCM simulations across Europe, highlighting distinct correlation patterns, particularly in Central Europe. Miralles et al. (2011) validated GLEAM using FLUXNET data, reporting good agreement (R = 0.86 at the daily scale and R = 0.94 at the monthly scale). These studies also emphasize the variable performance and applicability of the evapotranspiration datasets across Europe.

Conclusion

Our earlier analyses indicated changes in the hydrological cycle in the Jalovecký Creek catchment after 2014 (e.g. Holko et al., 2020). While the AET calculated from the hydrological balance showed the decrease in period 2014–2019, the AET simulated by two spatially distributed hydrological models and data from the remote sensing, did not indicate such a decreases. Despite interesting numbers on the AET simulated for different vegetation zones, only a small number of years (2 for WaSiM, 1 for MIKE SHE) were found when the simulated annual catchment runoff and AET differed from the measured runoff and AET calculated from the water balance equation by less than 10% (i.e. the results could be considered reasonable).

The AET estimates from reanalyses and satellite datasets also exhibited lower interannual variability than those derived from the hydrological balance. ERA5 systematically underestimated monthly AET (by up to 40%) compared to other datasets, while MERRA2 consistently provided values at the upper end (up to 30–40% higher than ERA5 in summer). Although spatial data from the products based on the remote sensing can provide valuable information for the larger scale studies, the values extracted for our small study catchment (for the analysis of interannual variability), should be taken with care. The study compared AET estimates from hydrological models with those from reanalysis and satellite datasets, rather than with direct observations. The lack of in-situ measurements (e.g., sap flow, eddy-covariance/turbulent fluxes, or other field experiments) limits the ability to validate both the interannual variability and the spatial patterns.

Acknowledgement

This study was supported by the grants from the Slovak Academy of Sciences (project VEGA No. 2/0019/23) and Slovak Research and Development Agency (projects No. APVV-23-0332 and VV-MVP-24-0208).

References

Dee, D. P., Uppala, S. M., Simmons, A. J., Berrisford, P., Poli, P., Kobayashi, S., Andrae, U., Balmaseda, M. A., Balsamo, G., Bauer, P., Bechtold, P., Beljaars, A. C. M., van de Berg, L., Bidlot, J., Bormann, N., Delsol, C., Dragani, R., Fuentes, M., Geer, A. J., Haimberger, L., Healy, S. B., Hersbach, H., Hólm, E. V., Isaksen, L., Kållberg, P., Köhler, M., Matricardi, M., McNally, A. P., Monge-Sanz, B. M., Morcrette, J.-J., Park, B.-K., Peubey, C., de Rosnay, P., Tavolato, C., Thépaut, J.-N., Vitart, F. (2011): The ERA-Interim reanalysis: Configuration and performance of the data assimilation system. Quarterly Journal of the Royal Meteorological Society, 137, 656, 553–597. https://doi.org/10.1002/qj.828.

Doherty, J. (2016): PEST Model-Independent Parameter Estimation User Manual Part I, 6th ed.; Watermark Numerical Computing: Brisbane, Australia.

Duan, Q. Y., Gupta, V. K, Sorooshian, S. (1993): Shuffled complex evolution approach for effective and efficient global minimization. J. Optimization Theory and Appl. 76, 3, 501–521.

Duethmann, D., Blöschl G. (2018): Why has catchment evaporation increased in the past 40 years? A data-based study in Austria. 2018. Hydrology Earth System Sciences, 22, 10, 5143–5158.

Gao, H., Tang, Q., Ferguson, C. R., Wood, E. F., Lettenmaier, D. P. (2010): Estimating the water budget of major US river basins via remote sensing. International Journal of Remote Sensing 31, 14, 3955–3978.

Gelaro, R., McCarty, W., Suárez, M., Todling, R., Molod, A., Takacs, L., Randles, C., Darmenov, A., Bosilovich, M., Reichle, R., Wargan, K., Coy, L., Cullather, R., Draper, C., Akella, S., Buchard, V., Conaty, A., da Silva, A., Gu, W., Kim, G., Koster, R., Lucchesi, R., Merkova, D., Nielsen, J., Partyka, G., Pawson, S., Putman, W., Rienecker, M., Schubert, S., Sienkiewicz, M., Zhao, B. (2017): The modern-era retrospective analysis for research and applications, version 2 (MERRA-2). Journal of Climate, 30, 14, 5419–5454. https://doi.org/10.1175/JCLI-D-16-0758.1.

Global Modeling and Assimilation Office (GMAO) (2015): M2T1NXLND. Greenbelt: Goddard Earth Sciences Data and Information Services Center (GES DISC).

Hlaváčiková, H., Novák, V., Orfánus, T., Danko, M., Hlavčo, J. (2014): Hydrofyzikálne charakteristiky skeletnatých pôd I. hydraulické vodivosti. Acta Hydrologica Slovaca, 15, 1, 24–34. (in Slovak)

Holko, L., Danko, M., Sleziak, P. (2020): Analysis of changes in hydrological cycle of a pristine mountain catchment. 2. Isotopic data, trend and attribution analyses. J. Hydrol. Hydromech., 68, 2020, 2, 192–199. DOI: 10.2478/johh-2020-0011

Hu, Z., Wang, G., Sun, X., Huang, K., Song, Ch., Yang. L., Sun, S., Sun, J., Lin, S. (2024): Energy partitioning and controlling factors of evapotranspiration in an alpine meadow in the permafrost region of the Qinghai-Tibet Plateau. Journal of Plant Ecology. https://doi.org/10.1093/jpe/rtae002.

Huang, Y., Hendricks Franssen, H., Herbst, M., Hirschi, M., Michel, D., Seneviratne, S.I., Teuling, A.J., Vogt, R., Schumacher, D., Pütz, T., Vereecken, H. (2020): Evaluation of different methods for gap filling of long-term actual evapotranspiration time series measured by lysimeters. Vadose Zone Journal, 19. https://doi.org/10.1002/vzj2.20020.

Jančo, M., Danko, M., Sleziak, P., Holko, L. (2024): Estimation of the leaf area index in a decline spruce forest in the Western Tatra Mountains for determination of rainfall interception. Acta Hydrologica Slovaca, 25, 1, 106-114.

Jin, X., Jin, Y. (2020): Calibration of a distributed hydrological model in a data-scarce basin based on GLEAM datasets. Water, 12, 3. https://doi.org/10.3390/w12030897.

Kantor, P. (1984): Vodohospodářská funkce horských smrkových a bukových porostů. Lesnictví, 30, 6, 471–490.

Knist, S., Goergen, K., Buonomo, E., Christensen, O. B., Colette, A., Cardoso, R. M., Fealy, R., Fernández, J., García-Díez, M., Jacob, D., Kartsios, S., Katragkou, E., Keuler, K., Mayer, S., Meijgaard, E., Nikulin, G., Soares, P. M. M., Sobolowski, S., Szepszo, G., Teichmann, C., Vautard, R., Warrach-Sagi, K., Wulfmeyer, V., Simmer, C. (2017): Land-atmosphere coupling in EURO-CORDEX evaluation experiments. Journal of Geophysical Research, 122, 1, 79–103. https://doi.org/10.1002/2016JD025476.

Ma, Q., Li, Y., Liu, F., Feng, H., Biswas, A., Zhang, Q. (2023): SPEI and multi-threshold run theory based drought analysis using multi-source products in China. Journal of Hydrology, 616, 128737. https://doi.org/10.1016/

j.jhydrol.2022.128737.

MIKE by DHI (2011): MIKE SHE. An integrated hydrological modeling framework. Vol. 2. Refer. Manual, p. 444.

Miralles, D. G., Holmes, T. R. H., De Jeu, R. A. M., Gash, J. H., Meesters, A. G. C. A., Dolman, A. J. (2011): Global land-surface evaporation estimated from satellite-based observations. Hydrology and Earth System Sciences, 15, 2. https://doi.org/10.5194/hess-15-453-2011.

Monteith, J. L. (1975): Vegetation and the atmosphere. Vol 1: Principles. Academic Press, London.

Nakai, Kim, Y., Busey, R., Suzuki, R., Nagain, S., Kobayashi, H., Park, H., Sugiura, K., Ito, A. (2013): Characteristics of evapotranspiration from a permafrost black spruce forest in interior Alaska. Polar Science, 7, 2, 136–148.

Nash, J. E., Sutcliffe, J. V. (1970): River flow forecasting through conceptual models part I-A discussion of principles. Journal of Hydrology, 10, 3, 282–290.

Parajka, J., Szolgay J., Mészároš, I., Kostka, Z. (2004): Grid-based mapping of the long-term mean annual potential and actual evapotranspiration in upper Hron river basin, J. Hydrol. Hydromech., 52, 4, 7–8.

Pekárová, P., Vyshnevskyi, V., Pekár, J., Miklánek, P. (2023): Changes in water balance components of river basins in the Slovak Republic and Ukraine. Acta Hydrologica Slovaca, 24, 1, 113–121.

Reichle, R. H., Koster, R. D., De Lannoy, G. J. M., Forman, B. A., Liu, Q., Mahanama, S. P. P., Touré, A. (2011): Assessment and enhancement of MERRA land surface hydrology estimates. Journal of Climate, 24, 24, 6322–6338. https://doi.org/10.1175/JCLI-D-10-05033.1.

Rodell, M., Houser, P. R., Jambor, U., Gottschalck, J., Mitchell, K., Meng, C., Arsenault, K., Cosgrove, B., Radakovich, J., Bosilovich, M., Entin, J. K., Walker, J. P., Lohmann, D., Toll, D. (2004): The Global Land Data Assimilation System. Bulletin of the American Meteorological Society, 85, 3, 381–394. https://doi.org/10.1175/BAMS-85-3-381.

Rui, H. L., Beaudoing, H. (2020): README Document for NASA GLDAS Version 2 Data Products. Goddard Earth Sciences Data and Information Services Center (GES DISC), 16, 1.

Salazar-Martínez, D., Holwerda, F., Holmes, T. R. H., Yépez, E. A., Hain, C. R., Alvarado-Barrientos, S., Ángeles-Pérez, G., Arredondo-Moreno, T., Delgado-Balbuena, J., Figueroa-Espinoza, B., Garatuza-Payán, J., González del Castillo, E., Rodríguez, J. C., Rojas-Robles, N. E., Uuh-Sonda, J. M., Vivoni, E. R. (2022): Evaluation of remote sensing-based evapotranspiration products at low-latitude eddy covariance sites. Journal of Hydrology, 610. https://doi.org/10.1016/j.jhydrol.2022.127786.

Schrödter, H. (1985): Verdunstung - Anwendungsorientierte Meßverfahren und Bestimmungsmethoden. Springer Verlag. (in German)

Schulla, J. (2019): Model Description WaSiM (Water Balance Simulation Model). Last change: November 9, 2019 (version 10.04.07), Hydrology Software Consulting J. SchullaRegensdorferstrasse 162CH 8049 Zürich. 376 pp.

Schulla, J. (1997): Hydrologische Modellierung von Flussgebieten zur Abschätzung der Folgen von Klimaänderungen. Zürcher Geographische Schriften, Heft 69, ETH Zürich, 161 pp. (in German)

Somorowska, U. (2022): Changes in Terrestrial Evaporation across Poland over the Past Four Decades Dominated by Increases in Summer Months. Resources, 11, 1. https://doi.org/10.3390/resources11010006.

Takacs, L. L., Suárez, M. J., Todling, R. (2016): Maintaining atmospheric mass and water balance in reanalyses. Quarterly Journal of the Royal Meteorological Society, 142, 697. https://doi.org/10.1002/qj.2763.

Talsma, C. J., Good, S. P., Miralles, D. G., Fisher, J. B., Martens, B., Jimenez, C., Purdy, A. J. (2018): Sensitivity of evapotranspiration components in remote sensing-based models. Remote Sensing, 10, 10. https://doi.org/10.3390/rs10101601.

Yan, H., Huang, J., He, Y., Liu, Y., Wang, T., Li, J. (2020): Atmospheric water vapor budget and its long-term trend over the Tibetan Plateau. Journal of Geophysical Research: Atmospheres, 125, 23. https://doi.org/10.1029/2020JD033297.

Zhang, K., Kimball, J. S., Running, S. W. (2016): A review of remote sensing based actual evapotranspiration estimation. In Wiley Interdisciplinary Reviews: Water, 3, 6. https://doi.org/10.1002/wat2.1168

Zhang, K., Kimball, J. S., Nemani, R. R., Running, S. W. (2010): A continuous satellite-derived global record of land surface evapotranspiration from 1983 to 2006. Water Resour. Res. 46, 9.

Zhu, G., Lu, L., Su, Y., Wang, X., Cui, X., Ma, J., He, J., Zhang, K., Li, Ch. (2014): Energyflux partitioning and evapotranspiration in a sub-alpine spruce forest ecosystem. Hydrol. Process. 28, 5093–5104.

Ing. et Ing. Patrik Sleziak, PhD. (*corresponding author, e-mail: sleziak@uh.savba.sk)
Ing. Michal Danko, PhD.
Ing. Martin Jančo, PhD.
RNDr. Ladislav Holko, CSc.
Institute of Hydrology SAS
Dúbravská cesta 9, 841 04 Bratislava
Slovak Republic

Ing. Viera Rattayová, PhD.
Slovak Hydrometeorological Institute
Climatological Service Department
Jeséniova 17, 833 15 Bratislava
Slovak Republic